applied sciences

MDPI

Article

Could the Enrichment of a Biomaterial with Conditioned Medium or Extracellular Vesicles Modify Bone-Remodeling Kinetics during a Defect Healing? Evaluations on Rat Calvaria with Synchrotron-Based Microtomography

Alessandra Giuliani [1,*], Gabriela Sena [2], Giuliana Tromba [3], Emanuela Mazzon [4], Antonella Fontana [5], Francesca Diomede [6], Adriano Piattelli [6] and Oriana Trubiani [6]

1 Department of Clinical Sciences, Polytechnic University of Marche, Ancona 60131, Italy
2 COPPE, Federal University of Rio de Janeiro, Rio de Janeiro 999074, Brazil; gabisenaa@gmail.com
3 Elettra Sincrotrone Trieste S.C.p.A, 34149 Trieste, Italy; giuliana.tromba@elettra.eu
4 IRCCS Centro Neurolesi "Bonino Pulejo", 98124 Messina, Italy; emazzon.irccs@gmail.com
5 Department of Pharmacy, University "G. d'Annunzio", 66100 Chieti, Italy; antonella.fontana@unich.it
6 Department of Medical Oral and Biotechnological Sciences, "G. d'Annunzio", 66100 Chieti, Italy; francesca.diomede@unich.it (F.D.); apiattelli@unich.it (A.P.); trubiani@unich.it (O.T.)
* Correspondence: a.giuliani@univpm.it; Tel.: +39-0712204603

Received: 5 February 2020; Accepted: 27 March 2020; Published: 29 March 2020

Featured Application: We showed, for the first time to the authors' knowledge, that mesenchymal stem cells derivatives, such as conditioned medium and extracellular vesicles, when seeded on collagen membranes or poly-(lactide) biomaterials, substantially accelerate bone-remodeling kinetics during defect healing. The study was performed by synchrotron radiation-based high-resolution tomography, focusing on the analysis of bone mass density distribution (BMDD). We showed the appropriateness of the proposed method to sensitively measure BMDD in bone-regenerated tissues; indeed, the same method was previously applied only in the evaluation of diagnosis and treatment of bone diseases. In this context, the scientific interest of this study is related to the use of oral stem cells, their engineered and not engineered derivatives, in the regeneration of the skeletal segment.

Abstract: Tissue engineering has been shown to offer promising approaches for bone regeneration, mostly based on replacement with biomaterials that provide specific environments and support for bone growth. In this context, we previously showed that mesenchymal stem cells (MSCs) and their derivatives, such as conditioned medium (CM) and extracellular vesicles (EV), when seeded on collagen membranes (COL) or polylactide (PLA) biomaterials, are able to favor bone tissue regeneration, especially evidenced in animal model calvary defects. In the present study, we investigated whether the enrichment of a rat calvary defect site with CM, EVs and polyethylenimine (PEI)-engineered EVs could substantially modify the bone remodeling kinetics during defect healing, as these products were reported to favor bone regeneration. In particular, we focused the study, performed by synchrotron radiation-based high-resolution tomography, on the analysis of the bone mass density distribution. We proved that the enrichment of a defect site with CM, EVs and PEI-EVs substantially modifies, often accelerating, bone remodeling kinetics and the related mineralization process during defect healing. Moreover, different biomaterials (COL or PLA) in combination with stem cells of different origin (namely, human periodontal ligament stem cells-hPDLSCs and human gingival mesenchymal stem cells-hGMSCs) and their own CM, EVs and PEI-EVs products were shown to exhibit different mineralization kinetics.

Keywords: conditioned medium; extracellular vesicles; bone-remodeling kinetics; healing; synchrotron-based microtomography

1. Introduction

Mineralized bone is a fundamental connective tissue because it supports locomotion, protects the soft tissues and is the reserve of calcium and phosphate in the human body. It is highly remodeled thanks to a process that combines resorption due to osteoclasts and bone formation due to osteoblasts [1].

However, when large bone defects are present due to trauma or skeletal anomalies or when a disease causes an unbalanced regenerative process, as in the case of osteoporosis, bone regeneration is an important issue that requires specific treatments. In these cases, tissue engineering has been shown to offer promising approaches for bone regeneration, most of which are based on replacement with biomaterials that provide specific environments that promote bone formation. The ideal biomaterial should not only be biocompatible and safe, but should be osteoinductive and osteoconductive, also improving cell viability, adhesion, proliferation and osteogenic differentiation [2,3].

Several biomaterials have been used for bone repair, such as collagen membranes (3D-COL) and polylactide (PLA). 3D-COL membranes have already been used in guided bone regeneration surgery, mainly for maxillofacial regeneration, for instance, to enclose the repaired site filled with bone autograft and promote faster bone healing [4,5]. As shown in studies on animal models and in clinical applications for the regeneration of dental tissues, the composition and structure of these membranes are of fundamental interest as they influence the effectiveness of bone regeneration [5]. Bio-resorbable membranes made with natural materials, such as collagen and chitosan, have been shown to have excellent biocompatibility; however, they have different mechanical properties, with some of them having a very rapid degradation rate in vivo. In fact, a relatively rapid degradation of barrier membranes has proved to be a cause of spontaneous periodontal healing [6]. PLA is a hydrophobic aliphatic polyester with several biomedical and clinical applications [7]; it is one of the most used biomaterials in regenerative medicine because of its characteristics, as both PLA and its degradation products are biocompatible and safe [8]. For these reasons, PLA was successfully used to realize scaffolds for bone and osteochondral regeneration [9,10].

The scaffolds can be cultured with cells, such as mesenchymal stem cells (MSCs), favoring bone regeneration through differentiation towards the osteogenic lineage or through the release of specific soluble factors. Alternatively, it is possible to functionalize the scaffolds with soluble molecules, which can then be released into the site to be regenerated, performing a therapeutic action [3]. In particular, MSCs are widely used in regenerative medicine as they can be recruited in different body districts, including dental tissues, and because of their multilineage differentiation potential [11]. In case of bone tissue engineering, MSC's ability to differentiate into osteoblasts has been widely studied [12]. Moreover, even if most of the studies were focused on bone marrow-derived MSCs, MSCs derived from other sites could offer some advantages, as in the case of MSCs derived from dental tissues, that can be easily isolated and have shown good performances in bone regeneration [13–15]. We have shown that these MSCs and their derivatives, such as conditioned medium (CM) and extracellular vesicles (EV), when seeded on appropriate biomaterials, are able to regenerate bone tissues, especially in calvary defects [16–20].

Among oral-derived MSCs, periodontal ligament (PDLSCs) and gingival (GMSCs) MSCs showed excellent performances in bone regeneration [16–24]. PDLSCs are very challenging in bone tissue engineering, showing a high capacity to proliferate, immunomodulatory competencies, ability to differentiate into osteogenic lineages, and also generating new bone after ectopic transplantation [25–28]. GMSCs offer other advantages: they are easy to isolate without requiring invasive procedures, proliferate fast and homogenously, maintaining stable morphology, normal karyotype and properties in time [29].

However, another advantage in using MSCs for bone engineering is linked to their capacity to release different factors, including growth factors, soluble proteins and free nucleic acids [30]; specifically, the conditioned medium (CM) contains different growth factors secreted by MSCs, possibly very useful for regenerative purposes, as recently shown [31] with special reference to bone regeneration [32–35].

In addition, the extracellular vesicles (EVs) released by MSCs, in particular the exosomes, were proved to offer great potential in regenerative medicine [36,37], including a positive regulation of osteoblastic differentiation [38]. Indeed, several studies reported the MSC-derived EV capacity to increase both bone-defect healing and osteochondral regeneration [39,40].

Moreover, in recent studies, we also tested polyethylenimine (PEI)-engineered EVs. PEI is a synthetic polymer that has been shown to possess low toxicity and high biological activity, forming non-convalent complexes with the DNA, which can be efficiently taken up by cells through endocytosis [41]. Moreover, PEI is able to induce the intracellular release of PEI–nucleic acid complexes from endosomes. Thus, PEI-EVs, obtained by non-covalently coating vesicles with PEI, were demonstrated to be internalized at the cytoplasmic level with higher efficiency when compared to EVs alone [16,20] probably by promoting the release of EV content into cells, and to favor fracture healing. Indeed, PEI behaves as a proton-sponge thus activating osmotic swelling that causes a burst of endosomes without the need for an additional endosomolytic agent.

The aim of this study was the investigation of the bone density distribution in-vivo, on rat calvaria defects, grafted with two alternative constructs: (a) COL scaffold seeded with human PDLSCs (hPDLSCs) and hPDLSCs-derived CM or hPDLSCs-derived EVs or hPDLSCs-derived PEI-EVs; (b) PLA scaffold enriched with human GMSCs (hGMSCs) and hGMSCs-derived CM or hGMSCs-derived EVs or hGMSCs-derived PEI-EVs.

We investigated whether the enrichment of the defect site with CM, EVs and PEI-EVs could substantially modify the bone remodeling kinetics during the defect healing, as these products were reported to favor bone regeneration. In particular, we focused the study, performed by synchrotron radiation-based high-resolution tomography, on the analysis of bone mass density distribution: this investigation, to our knowledge, has never been performed in these constructs.

2. Materials and Methods

2.1. Cell Culture

The Ethics Committee of the Medical School at the "G. d'Annunzio" University (Chieti, Italy) obtained informed consent for tissue collection from each participant. PDLSCs and their derivatives were obtained by healthy donors, removing the teeth for orthodontic purposes; GMSCs and their derivatives were obtained from gingival tissues of healthy adult donors, without gingival inflammation, as previously described by Diomede et al. [42].

2.2. Scaffolds

The first type of scaffold was a collagen membrane (COL) obtained from equine mesenchymal tissue (Evolution; Tecnoss®Dental, Giaveno, Italy). It is dense in fibers, ensuring easy suitability to nearby tissues and protecting underlying grafts. COL pieces of about 4×7 mm^2 were washed with sterile phosphate buffered saline (PBS) (Lonza, Basel, Switzerland) to rehydrate them before their grafting in-vivo.

The second type of scaffold was a polylactide scaffold (PLA) of commercial origin (Kaytech srl, Ancona, Italy), realized by a commercial CAD software (Rhinoceros 5, McNeel Europe, Barcelona, Spain) [18], with projects then applied to a printing slicing software (Cura 15.04, Ultimaker B.V., Geldermalsen, The Netherlands) that was finally transferred to a commercial 3D printer (DeltaWASP 2040; CSP srl, Massa Lombarda, Italy) [43].

2.3. Conditioned Medium (CM)

The CM was obtained from $15 \times 10^3/cm^2$ hSCs at the 2nd passage, after 48 h and 72 h of incubation for hPDLSCs and hGMSCs, respectively. Afterwards, the CM was centrifuged for 5 min at 1200 rpm in order to remove suspension cells and debris. The supernatants were recentrifuged for 3 min at 3000 rpm in order to collect the secondary supernatants. Then, 1 mL of secondary supernatants was resuspended in 3 mL of ice acetone and maintained overnight at 4 °C; then, it was recentrifuged for 12 min at 16000 rpm at 4 °C (Centrifuge 5804 R, Eppendorf, Milan, Italy) and the resulting suspension was lysated in radioimmunoprecipitation assay (RIPA) buffer and quantified by means of the Bradford assay [44]. The amount of proteins obtained in both cases was 125 µg/µL.

2.4. Extracellular Vesicles (EVs)

ExoQuick TC commercial agglutinant (System Biosciences, Palo Alto, CA, United States), in the quantity of 2 mL, was added to 10 mL of CM obtained from hPDLSCs or hGMSCs. The mixture was incubated overnight at 4 °C; afterwards, centrifugation was performed at 1500× *g* for 30 min to sediment the EVs that were then resuspended in 200 µl of PBS [18,45,46]. No further washing was performed in order to eliminate the agglutinating polymer.

2.5. Engineered Extracellular Vesicles (PEI-EVs)

Quotes of EVs were coated with branched polyethylenimine (PEI, MW 25,000 Sigma-Aldrich) by means of a non-covalent layer-by-layer protocol described in the literature [47,48]. Briefly, 100 µL of EVs, dispersed with 2 mL of PBS, were added to 2 mL of PEI dissolved in 0.3 M NaCl (PEI final concentration around 0.05 mg/mL) and incubated for 20 min at room temperature. The obtained suspension was centrifuged at 4000 rpm for 15 min, the excess of PEI and the residual polymer were removed and the precipitate was resuspended in 2 mL of PBS. Despite the initial dilution of resuspended EV and the final precipitation steps are assimilable to a washing step, the complete removal of agglutinating polymer cannot be ensured.

2.6. Animals and Ethics Statement for Animal Use

Male Wistar rats (Harlan Laboratories, Indianapolis, IN, USA), with a weight of 300–350 g, were used for this experiment. They were individually hosted in ventilated cages, with 12 h light/dark cycles, at a temperature of 21 ± 1 °C and humidity of 50–55%, with food and water ad libitum.

All animal experiments complied with the ARRIVE guidelines and were carried out in accordance with the EU Directive 2010/63/EU for animal experiments. The Ministry of Health "General Direction of animal health and veterinary drug" authorized the study (Authorization 768/2016-PR 28/07/2016-D.lgs 26/2014) that was planned in order to minimize the total number of rats sacrificed while maintaining statistical significance, as previously assessed [17,20].

2.7. Scaffold Grafting

Before scaffold grafting, the animals were first anesthetized (tiletamine and xylazine—10 mL/kg, intraperitoneal; i.p.); afterwards, the implant site was trichotomized, prepared with iodopovinone (Betadine) and then cut through the total thickness with a median sagittal incision of about 1.0 cm in the frontoparietal region. A circular bone defect was created (diameter of 5 mm; height of 0.25 mm) with a trephine milling machine (Alpha Bio-Tec, HTD Consulting S.r.l., Siena, Italy) equipped to supply constant irrigation with physiological solution.

The prepared constructs were easily grafted, assuring contact with bone defect border and the covering of the whole defect. The skin flap was then sutured using Caprosyn 6–0 synthetic monofilament absorbable sutures (Covidien AG, Neuhausen am Rheinfall, Switzerland) and, finally, the animals were maintained, up to sacrifice, with standard feeding and hydration.

2.8. Experimental Design

In the overall study, CM, EVs and PEI-EVs PBS solutions were seeded on biomaterials (COL or PLA) and maintained at 37 °C for 24 h. After this incubation, the enriched scaffolds were seeded with stem cells (hPDLSCs or hGMSCs). Subsequently, after the scraping of their cortical calvaria bone tissue, the rats were randomly distributed into 10 groups of study, each of them grafted with different combinations of biomaterials, stem cells and their derivatives.

Six weeks later, under anesthesia (tiletamine and zolazepam), the animals were euthanized by intravenous administration of Tanax (5 mL/kg body weight). Afterwords, their calvariae were excised and prepared for synchrotron-based high resolution tomographic (microCT) analysis.

2.9. Synchrotron Radiation microCT Examination

The microCT experiments were performed at the SYRMEP beamline of ELETTRA Synchrotron Facility (Basovizza-TS, Italy) using the following settings: 1800 projections, each with 0.4 s exposure time, over a total range of 180°; pink beam with peak energy at ~20 keV; sample-detector distance at ~65 mm, resulting in $(2.5\ \mu m)^3$ isotropic voxel size in reconstructed images. Because of the coherence characteristics of the synchrotron beam, the recorded radiographs included phase contrast signals. The approach was based on discrimination between attenuation properties, related to the absorption index β, and refractive index decrement δ of the index of refraction $n = 1 - \delta + i\beta$ in the newly-formed mineralized bone inside the defect. The reconstruction was performed using Paganin's method [49], where the phase is retrieved by assuming that the δ/β ratio is constant. This ratio was set to 100 in the present investigation.

The VG Studio MAX 1.2 (Volume Graphics, Heidelberg, Germany) software allowed to produce 3D images where mass density differences within samples translate into different peaks in the gray-level scale, corresponding to the different phases. The threshold of the histograms was manually set to 117 (8 bit scale: 0-255) for all the samples, separating the mineralized bone from soft tissues and scaffold phases. For each biopsy, two 3D subvolumes were analyzed: the former (test), with dimensions of $1.25 \times 1.25 \times 0.25\ mm^3$, was included in the defect bulk and the latter (ctr), with identical dimensions, in the same frontoparietal area but outside the defect.

We exploited the reconstructed refractive index n distribution [50], which is linearly related to mass density, to study the relative bone mass density distribution (MDD^r). The MDD^r parameters were calculated within the mineralized domain inside and outside the defect. We could not retrieve the absolute values of bone mass density (proportional to calcium concentrations—Ca weight %) because n would have possibly been biased on account of the chosen constant ratio δ/β [51]. However, since the different subvolumes were identical in terms of size and had a similar composition, the relative difference in mass density distribution between them could be appreciated; thus, hereinafter the superscript r will denote relative values for all the parameters. Following the Roschger approach [51], five parameters were extracted using the PeakFit software (Systat Software, San Jose, CA): the most frequent relative mass density value (MDD^r_{peak}), the mean relative mass density (MDD^r_{mean}), the full width at half maxima of the distribution (MDD^r_{fwhm}), the 0.5th (MDD^r_{low}) and the 99.5th (MDD^r_{high}) percentiles.

3. Results

Synchrotron-based high resolution tomographic (microCT) analyses were performed on rat calvaria of the following groups of study:

(1) COL (N = 4): rats grafted with COL;
(2) COL/hPDLSCs (N = 4): rats grafted with COL enriched with hPDLSCs;
(3) COL/hPDLSCs/CM (N = 4): rats grafted with COL enriched with hPDLSCs and CM;
(4) COL/hPDLSCs/EVs (N = 4): rats grafted with COL enriched with hPDLSCs and EVs;
(5) COL/hPDLSCs/PEI-EVs (N = 4): rats grafted with COL enriched with hPDLSCs and PEI-EVs;

(6) PLA (N = 4): rats grafted with PLA;
(7) PLA/hGMSCs (N = 4): rats grafted with PLA enriched with hGMSCs;
(8) PLA/hGMSCs/CM (N = 4): rats grafted with PLA enriched with hGMSCs and CM;
(9) PLA/hGMSCs/EVs (N = 4): rats grafted with PLA enriched with hGMSCs and EVs;
(10) PLA/hGMSCs/PEI-EVs (N = 4): rats grafted with PLA enriched with hGMSCs and PEI-EVs.

MicroCT images of chosen scaffolds and some representative repaired sites in retrieved samples are shown in Figure 1. The 3D reconstructions of the COL and the PLA scaffolds before grafting were shown in Figure 1a,d, respectively. Moreover, representative 3D reconstructions of defects grafted with the sole biomaterial (Figure 1b for the COL and Figure 1e for the PLA) and with the biomaterial seeded with stem cells and engineered extracellular vesicles were also shown (Figure 1c for the COL/hPDLSCs/PEI-EVs and Figure 1f for the PLA/hGMSCs/PEI-EVs). All tissues, except for mineralized bone and residual scaffolds, were made virtually transparent. From the simple 3D reconstructions of the repaired defects, volume mismatches in terms of the amount of newly formed bone were evident between defects grafted with the sole biomaterials and those also treated with stem cells and engineered extracellular vesicles. In particular, the latter showed greater volumes and connectivity of newly formed bone than the former group, in agreement with previous morphometric studies on the same samples [20].

However, the present study was focused on the study of the relative bone mineral density distribution (MDD^r), describing and quantifying the calcium concentration and distribution (weight %) in the different groups of study. Indeed, independently from the volumetric growth of the newly formed bone in the different conditions, it is fundamental to evaluate the mineral density of the regenerated bone, strictly related to the kinetics of bone remodeling, as very recently shown by some of the authors [50]. In particular, this study was performed with an approach proposed by Roschger [52] and was focused on the mineralized bone portion. The method was supported by the parameters indicated in Figure 2a. In order to verify the sensitivity of the method, we first studied the distribution of both the mean relative mass density (MDD^r_{mean}) and the full width at half maxima of the distribution (MDD^r_{fwhm}) in the whole set of *ctr* sites (outside the defect), as shown with the support of box plots in Figure 2b–c. The high variability of the mean and of the fwhm values is motivated by the extremely high sensitivity of the synchrotron-based phase-contrast microCT combined with the use of different rats having different MDD in the studied calvarial site.

Moreover, for the complete ctr and test sets of data, we plotted the dispersion graphs describing mean vs. fwhm dependency, the two regression equations and their coefficient of determination R^2 (Figure 2d). R^2 values were found to be extremely low (R^2_{ctr} = 0.07; R^2_{test} = 0.20); thus, the high variability of the mean and of the fwhm values combined to their low correlation motivated us to investigate, instead of the absolute indices, the following relative parameters in each rat included in the groups of study:

$$\Delta MDD^r{}_i = MDD^r{}_{i,ctr} - MDD^r{}_{i,test},$$

where *i* defines each parameter between peak, mean, fwhm, low and high.

The results deriving from this analysis are listed in Table 1 and described below.

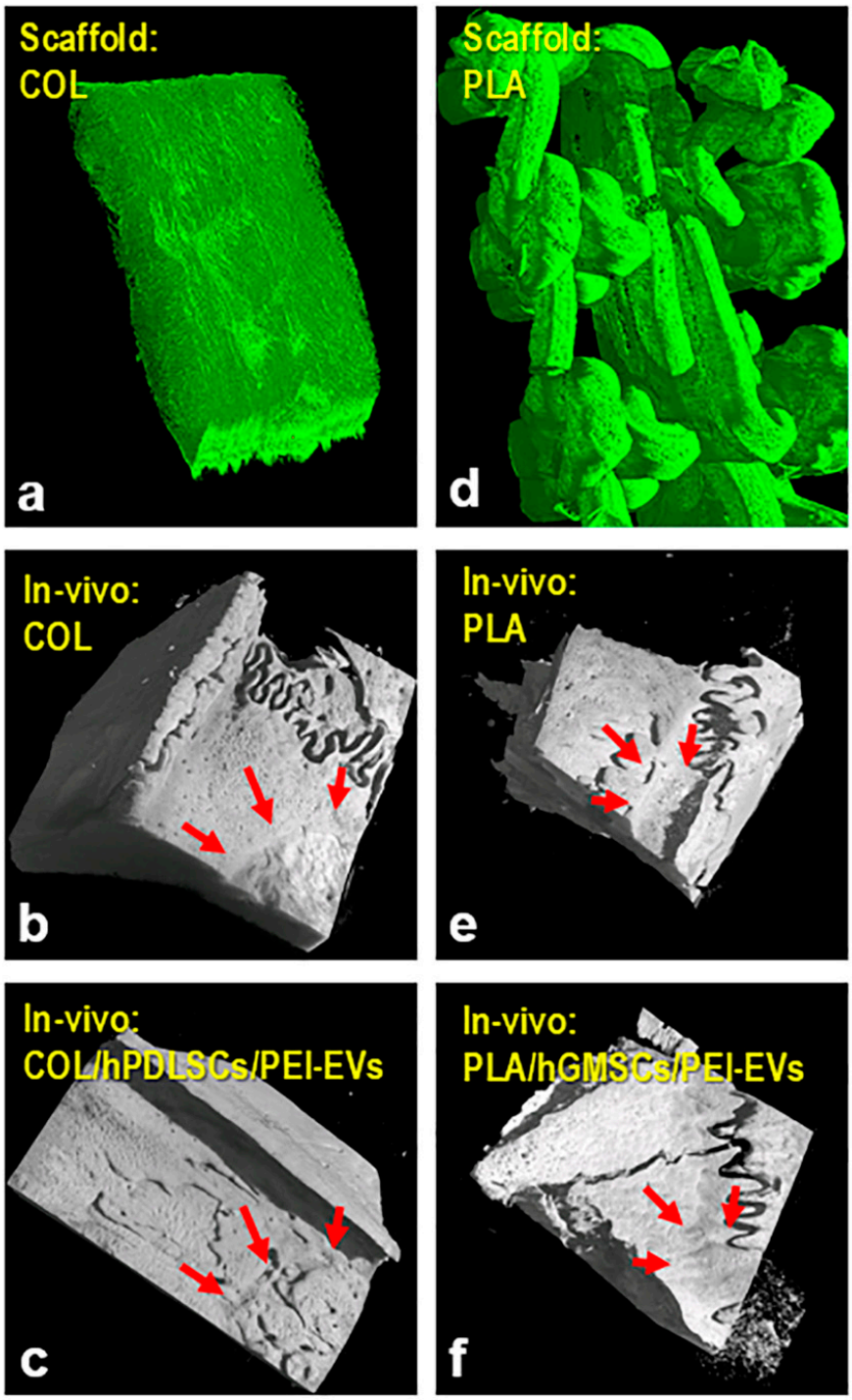

Figure 1. Phase-contrast MicroCT 3D images of representative samples. (**a**) Collagen membranes (COL) scaffold before grafting; (**b**,**c**) repaired calvarial defects: (**b**) representative sample of the COL group; (**c**) representative sample of the COL/hPDLSCs/PEI-EVs group; (**d**) poly-(lactide) scaffold (PLA) scaffold before grafting; (**e**,**f**) repaired calvarial defects: (**e**) representative sample of the PLA group; (**f**) representative sample of the PLA/hGMSCs/PEI-EVs group. Red arrows indicate the defect site in each panel. Phase-contrast signal (grey cloud of points) close to the defects repaired using PLA-based constructs represents PLA residuals.

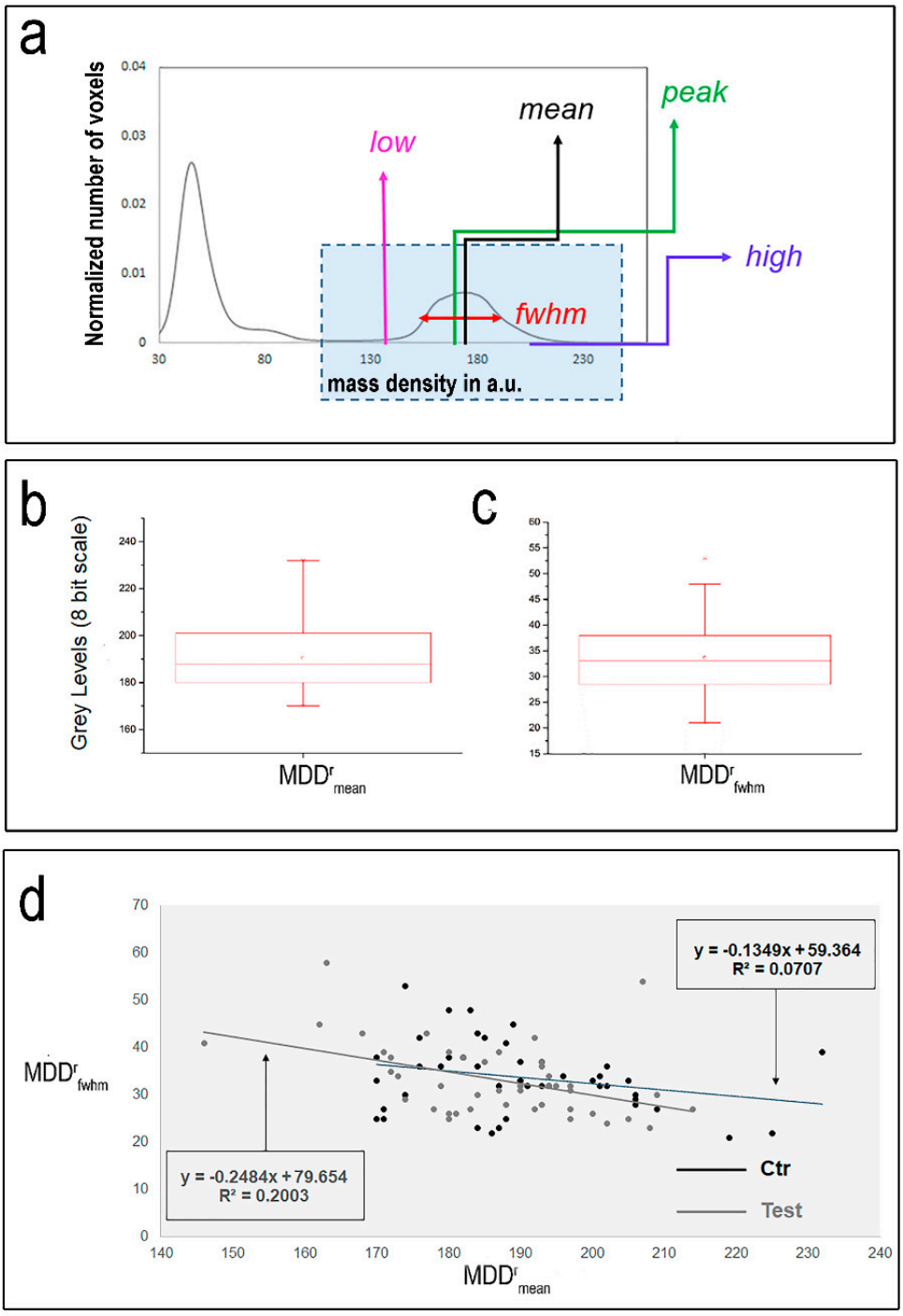

Figure 2. Parameters of interest for the analysis of bone relative mass density distribution (MDD^r). (**a**) Histogram of a representative sample: the peak on the right, highlighted in translucent blue, was referred to the overall mineralized bone that was regenerated into the defect. The parameters investigated with the Roschger approach are indicated. (**b**–**d**) Study of the sensitivity of the Roschger approach: box plots of the distribution (**b**) of the mean relative mass density (MDD^r_{mean}) and (**c**) of the full width at half maxima of the distribution (MDD^r_{fwhm}) in the whole set of *ctr* sites (i.e., in the calvaria but outside the defect); (**d**) dispersion graphs describing mean vs. fwhm dependency, the two regression equations and their coefficient of determination R^2 for the full sets of ctr and test data.

Table 1. Bone relative mass density distribution (MDD^r)—results. Instead of the absolute indices, the following relative parameters were studied in each rat included in the groups of study: $\Delta MDD^r{}_i = MDD^r{}_{i,ctr} - MDD^r{}_{i,test}$, where i defines each index between peak, mean, fwhm, low and high. Data are shown as mean (standard deviation) for each group of study.

	$\Delta MDD^r{}_{peak}$	$\Delta MDD^r{}_{mean}$	$\Delta MDD^r{}_{fwhm}$	$\Delta MDD^r{}_{low}$	$\Delta MDD^r{}_{high}$
COL	5.0 (4.3)	9.8 (5.6)	4.8 (3.4)	5.0 (2.8)	14.5 (8.8)
COL/hPDLSCs	−1.8 (1.1)	−1.3 (2.6)	4.8 (2.5)	−6.0 (0.3)	3.5 (5.1)
COL/hPDLSCs/CM	3.3 (3.9)	2.8 (3.8)	5.3 (1.4)	−2.5 (2.7)	8.0 (5.0)
COL/hPDLSCs/EVs	2.0 (9.7)	7.5 (8.6)	2.3 (6.6)	5.3 (2.9)	9.8 (15.1)
COL/hPDLSCs/PEI-EVs	−4.4 (0.6)	−1.4 (0.5)	0.4 (1.4)	−1.8 (1.1)	−1.0 (1.7)
PLA	4.8 (1.0)	6.5 (1.2)	0.5 (2.5)	6.0 (1.3)	7.0 (3.6)
PLA/hGMSCs	2.5 (1.9)	2.0 (2.9)	3.0 (3.3)	−1.0 (0.8)	5.0 (6.1)
PLA/hGMSCs/CM	−9.3 (3.9)	−8.5 (3.4)	−6.5 (2.8)	−2.0 (0.6)	−15.0 (6.3)
PLA/hGMSCs/EVs	5.3 (7.0)	10.3 (5.9)	0.5 (2.3)	9.8 (4.1)	10.8 (8.0)
PLA/hGMSCs/PEI-EVs	16.8 (6.8)	15.8 (6.8)	−11.0 (7.4)	26.8 (1.6)	4.8 (14.1)

Samples COL and PLA: the sole use of the biomaterial, regardless of its nature (COL or PLA), does not support complete regeneration either from a morphometric (volumetric) point of view, as previously observed [16–20], or from a comparison of the mineralization density distribution of test sites vs. control sites. Indeed, regenerated sites (test) in both the constructs presented positive values of $\Delta MDD^r{}_i$ for all the *i* variables (peak, mean, fwhm, low and high), indicating lower levels of mineralization than in *ctr* sites.

Samples COL/hPDLSCs and PLA/hGMSCs: the combination of biomaterials with the related stem cells has significantly improved the level of mineralization of the constructs. In any case, limited to the use of hPDLSCs, mineralization density distributions are still found shifted towards lower levels than in *ctr* sites, as suggested by the positive $\Delta MDD^r{}_{fwhm}$ combined to the negative $\Delta MDD^r{}_{low}$.

Samples COL/hPDLSCs/CM and PLA/hGMSCs/CM: the addition of the CM to the constructs, in the COL/hPDLSCs/CM samples, seemed to furtherly increase overlapping with the control sites, whereas in the case of PLA/hGMSCs/CM samples, they seemed to reach even higher levels of mineralization than the controls, with higher mean and variability values (negative $\Delta MDD^r{}_{mean}$ and negative $\Delta MDD^r{}_{fwhm}$, respectively) than control sites in the same calvariae.

Samples COL/hPDLSCs/EVs and PLA/hGMSCs/EVs: the substitution of the CM with the EVs did not seem to modify the mineralization distribution in the COL/hPDLSCs/EVs samples. Conversely, it appeared to be a less contributory choice in terms of mineralization in the case of use of PLA/hGMSCs/EVs constructs, where higher mean, low and high values (i.e., positive $\Delta MDD^r{}_{mean}$, $\Delta MDD^r{}_{low}$ and $\Delta MDD^r{}_{high}$) were found in the control sites than in the test sites of the same calvariae.

Samples COL/hPDLSCs/PEI-EVs and PLA/hGMSCs/PEI-EVs: in absolute terms, the use of engineered extracellular vesicles (PEI-EVs) appeared to be the most overlapping condition to the control sites, as resulted from the investigation of the COL/hPDLSCs/PEI-EVs samples, with the same $MDD^r{}_{mean}$, $MDD^r{}_{peak}$, $MDD^r{}_{low}$, $MDD^r{}_{high}$ and $MDD^r{}_{fwhm}$ values, considering the corresponding standard deviations. Conversely, in the case of PLA/hGMSCs/PEI-EVs samples, highly positive $\Delta MDD^r{}_{mean}$, $\Delta MDD^r{}_{low}$ and $\Delta MDD^r{}_{peak}$ values were found, suggesting the presence of lower mineralization levels than in ctr sites. However, highly negative $\Delta MDD^r{}_{fwhm}$ values were also found in the PLA/hGMSCs/PEI-EVs samples, indicating a wider density distribution in the test than in the ctr sites.

4. Discussion

Bone regeneration is still a challenge, particularly in maxillofacial sites. In this context, the use of biomaterials combined with stem cell cultures is giving promising results. Some of the authors of the present study have recently shown that scaffolds cultured with mesenchymal stem cells (MSC) and/or their derivatives, as conditioned medium (CM), extracellular vesicles (EV) or EV engineered with polyethylenimine (PEI-EV) improve bone regeneration. It is worth noting that EVs have been isolated, in the present as well as in the previous referred studies, by using ExoQuick TC commercial

agglutinant polymer. This means that the presence of residual agglutinating polymer cannot be excluded although, as reported in the Materials and Methods section, the engineering step could contribute to its removal and microscopic data [16,18] did not highlight the presence of polymer residue. Nevertheless, no evidence of cytotoxicity related to these residues has been evidenced [16,18] and Niu et al. [53] demonstrated that ExoQuick TC isolation preserves biological activities of EV. In particular, both in vitro and in vivo results on rat calvarial bone defects showed greater expression of osteogenic markers in scaffolds grown with human-derived SC and with PEI-EV, also associated with increased protein levels of vascular endothelial growth factor (VEGF) and VEGF 2 receptor (VEGFR2). Histological examination confirmed these deductions. Furthermore, the morphometric analysis deriving from microCT investigation confirmed on rat calvarial defects that scaffolds cultured with hSCs and PEI-EV exhibited increased bone regeneration and greater integration [20]. In this context, synchrotron radiation-based X-ray microtomography (microCT) has shown to be a powerful technique, able to achieve the analysis not only of bone microarchitecture but also of local mineralization at different hierarchical length scales, including the imaging of the lacuno–canalicular network [21,22,50,54].

Thus, in the present study, we introduced synchrotron microCT as an effective method to study bone regeneration and its remodeling, focusing the investigation on the bone mineral density distribution in rat calvarial defects grafted with two alternative constructs, namely COL scaffolds seeded with hPDLSCs, hPDLSCs + derived CM, hPDLSCs + derived EVs, or hPDLSCs + derived PEI-EVs, and PLA scaffolds enriched with hGMSCs, hGMSCs + derived CM, hGMSCs + derived EVs, or hGMSCs + derived PEI-EVs. The study of the mineralized bone density distribution was performed with the support of the innovative Roschger approach [52], as previously successfully achieved in different studies by some of the authors [50,54].

The mineralized bone density distribution analysis with synchrotron-based microCT showed increased mineralization in COL/hPDLSCs/PEI-EVs compared to other groups based on the same biomaterial and stem cells. Thus, not only bone morphometric analysis with microCT evidenced better bone regeneration in COL/hPDLSCs/PEI-EVs from a quantitative point of view [20] but the present study has contributed to assuring that their calcium content and distribution mimic better the control sites than all the other groups that grafted defects with the other COL-based constructs.

Conversely, a different scenario was found in the case of PLA/hGMSCs/PEI-EVs, showing not only the presence of lower mineralization levels but also a wider density distribution variance than in the control sites. This result can be justified, considering for these samples different bone remodeling kinetics. Indeed, as shown in the representative microCT sections of Figure 3, the network in the test sites, close to the PLA scaffold, appeared to be much denser of osteocyte lacunae than in the corresponding ctr sites. Furthermore, the lacunae were found to be larger in size in test sites, suggesting a recent change from the osteoblast condition and suggesting longer times to complete the mineralization process than six weeks from grafting, as experienced in the present study.

However, PLA/hGMSCs/CM samples were shown to reach levels of mineralization higher than the controls, with higher mean and variability values. This result completes the analysis on the conditioned medium performances recently started [17], where PLA/hGMSCs/CM showed a better osteogenic performance compared to constructs without CM; this was verified not only in vitro, by transcriptomic analysis, observing in the 3D-PLA + CM + hGMSCs group the upregulation of genes involved in ossification and regulation of ossification, but also in-vivo, efficiently repairing calvarial defects as revealed by histomorphometric evaluation.

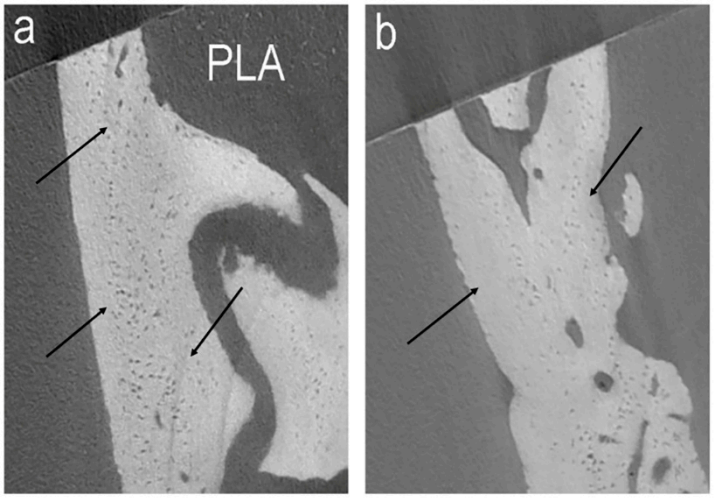

Figure 3. Evidence of bone remodeling kinetics. Representative microCT transversal sections of a PLA/hGMSCs/PEI-EVs sample in (**a**) test and (**b**) ctr sites. As shown by the arrows, in the *test* sites and close to the PLA residuals, bone appeared to be much denser of osteocyte lacunae than in the corresponding *ctr* sites, showing increased remodeling.

5. Conclusions

With the present study, we definitely proved that the enrichment of a defect site with CM, EVs and PEI-EVs substantially modifies, often accelerating, bone remodeling kinetics and the related mineralization process during defect healing. Moreover, different biomaterials (COL or PLA) in combination with stem cells of different origin (hPDLSCs or hGMSCs) and their own CM, EVs and PEI-EVs products were shown to exhibit different mineralization kinetics. Indeed, after six weeks from grafting in a calvarial defect, while increased mineralization was found in COL/hPDLSCs/PEI-EVs compared to the other COL-based groups, PLA/hGMSCs/PEI-EVs showed the presence of lower mineralization levels than some of the other PLA-based groups. However, PLA/hGMSCs/PEI-EVs had also a wider density distribution variance than in the control sites, suggesting the need of longer times for completing the mineralization process. Conversely, PLA/hGMSCs/CM samples were shown to reach high levels of mineralization, confirming better osteogenic capacity than constructs without the conditioned medium, as shown in previous studies.

Author Contributions: conceptualization, A.G. and O.T.; data curation, E.M., A.F. and O.T.; formal analysis, A.G.; funding acquisition, A.P. and O.T.; investigation, A.G., G.S., G.T. and F.D.; methodology, A.G., G.S. and G.T.; project administration, A.P.; resources, E.M., A.F. and F.D.; software, A.G. and G.S.; supervision, E.M., A.P. and O.T.; validation, A.G., A.F., F.D. and O.T.; writing—original draft, A.G. and O.T.; writing—review and editing, ALL. All authors have read and agreed to the published version of the manuscript.

Funding: The ELETTRA synchrotron experiments were funded by the Program "Support to the Italian Users of ELETTRA". This research received no external funding.

Acknowledgments: Authors thank the ELETTRA Synchrotron Facility for the allocated beamtime at the SYRMEP beamline. Authors also thank Jiaojiao Zhang for technical support during imaging data elaboration.

Conflicts of Interest: The authors declare no conflict of interest.

References

1. Florencio-Silva, R.; Sasso, G.R.; Sasso-Cerri, E.; Simoes, M.J.; Cerri, P.S. Biology of bone tissue: Structure, function, and factors that influence bone cells. *BioMed. Res. Int.* **2015**, *2015*, 421746. [CrossRef] [PubMed]
2. Wu, T.; Yu, S.; Chen, D.; Wang, Y. Bionic design, materials and performance of bone tissue scaffolds. *Materials* **2017**, *10*, 1187. [CrossRef] [PubMed]

3. Roseti, L.; Parisi, V.; Petretta, M.; Cavallo, C.; Desando, G.; Bartolotti, I.; Grigolo, B. Scaffolds for bone tissue engineering: State of the art and new perspectives. *Mater. Sci. Eng. C Mater. Biol. Appl.* **2017**, *78*, 1246–1262. [CrossRef] [PubMed]
4. El-Jawhari, J.J.; Moisley, K.; Jones, E.; Giannoudis, P.V. A crosslinked collagen membrane versus a non-crosslinked bilayer collagen membrane for supporting osteogenic functions of human bone marrow-multipotent stromal cells. *Eur. Cells Mater.* **2019**, *37*, 292–309. [CrossRef] [PubMed]
5. Dimitriou, R.; Mataliotakis, G.I.; Calori, G.M.; Giannoudis, P.V. The role of barrier membranes for guided bone regeneration and restoration of large bone defects: Current experimental and clinical evidence. *BMC Med.* **2012**, *10*, 81. [CrossRef] [PubMed]
6. Elgali, I.; Omar, O.; Dahlin, C.; Thomsen, P. Guided bone regeneration: Materials and biological mechanisms revisited. *Eur. J. Oral Sci.* **2017**, *125*, 315–337. [CrossRef]
7. Tyler, B.; Gullotti, D.; Mangraviti, A.; Utsuki, T.; Brem, H. Polylactic acid (pla) controlled delivery carriers for biomedical applications. *Adv. Drug Deliv. Rev.* **2016**, *107*, 163–175. [CrossRef]
8. Farah, S.; Anderson, D.G.; Langer, R. Physical and mechanical properties of pla, and their functions in widespread applications—A comprehensive review. *Adv. Drug Deliv. Rev.* **2016**, *107*, 367–392. [CrossRef]
9. Holmes, B.; Zhu, W.; Li, J.; Lee, J.D.; Zhang, L.G. Development of novel three-dimensional printed scaffolds for osteochondral regeneration. *Tissue Eng. Part* **2015**, *21*, 403–415. [CrossRef]
10. Gregor, A.; Filova, E.; Novak, M.; Kronek, J.; Chlup, H.; Buzgo, M.; Blahnová, V.; Lukášová, V.; Bartoš, M.; Nečas, A.; et al. Designing of pla scaffolds for bone tissue replacement fabricated by ordinary commercial 3d printer. *J. Biol. Eng.* **2017**, *11*, 31. [CrossRef]
11. Mushahary, D.; Spittler, A.; Kasper, C.; Weber, V.; Charwat, V. Isolation, cultivation, and characterization of human mesenchymal stem cells. *Cytometry A* **2018**, *93*, 19–31. [CrossRef] [PubMed]
12. Dominici, M.; Le Blanc, K.; Mueller, I.; Slaper-Cortenbach, I.; Marini, F.; Krause, D.; Deans, R.; Keating, A.; Prockop, D.; Horwitz, E. Minimal criteria for defining multipotent mesenchymal stromal cells.The international society for cellular therapy position statement. *Cytotherapy* **2006**, *8*, 315–317. [CrossRef] [PubMed]
13. Liu, J.; Yu, F.; Sun, Y.; Jiang, B.; Zhang, W.; Yang, J.; Xu, G.T.; Liang, A.; Liu, S. Concise reviews: Characteristics and potential applications of human dental tissue-derived mesenchymal stem cells. *Stem Cells* **2015**, *33*, 627–638. [CrossRef] [PubMed]
14. Fawzy El-Sayed, K.M.; Dorfer, C.E. Gingival mesenchymal stem/progenitor cells: A unique tissue engineering gem. *Stem Cells Int.* **2016**, *2016*, 7154327. [CrossRef] [PubMed]
15. Asutay, F.; Acar, H.A.; Yolcu, U.; Kirtay, M.; Alan, H. Dental stem cell sources and their potentials for bone tissue engineering. *J. Istanb. Univ. Fac. Dent.* **2015**, *49*, 51–56. [CrossRef]
16. Diomede, F.; D'Aurora, M.; Gugliandolo, A.; Merciaro, I.; Ettorre, V.; Bramanti, A.; Piattelli, A.; Gatta, V.; Mazzon, E.; Fontana, A.; et al. A novel role in skeletal segment regeneration of extracellular vesicles released from periodontal-ligament stem cells. *Int. J. Nanomed.* **2018**, *13*, 3805–3825. [CrossRef]
17. Diomede, F.; D'Aurora, M.; Gugliandolo, A.; Merciaro, I.; Orsini, T.; Gatta, V.; Piattelli, A.; Trubiani, O.; Mazzon, E. Biofunctionalized scaffold in bone tissue repair. *Int. J. Mol. Sci.* **2018**, *19*, 1022. [CrossRef]
18. Diomede, F.; Gugliandolo, A.; Cardelli, P.; Merciaro, I.; Ettorre, V.; Traini, T.; Bedini, R.; Scionti, D.; Bramanti, A.; Nanci, A.; et al. Three-dimensional printed PLA scaffold and human gingival stem cell derived extracellular vesicles: A new tool for bone defect repair. *Stem Cell Res. Ther.* **2018**, *9*, 104. [CrossRef]
19. Diomede, F.; Gugliandolo, A.; Scionti, D.; Merciaro, I.; Cavalcanti, M.F.; Mazzon, E.; Trubiani, O. Biotherapeutic effect of gingival stem cells conditioned medium in bone tissue restoration. *Int. J. Mol. Sci.* **2018**, *19*, 329. [CrossRef]
20. Pizzicannella, J.; Gugliandolo, A.; Orsini, T.; Fontana, A.; Ventrella, A.; Mazzon, E.; Bramanti, P.; Diomede, F.; Trubiani, O. Engineered Extracellular Vesicles From Human Periodontal-Ligament Stem Cells Increase VEGF/VEGFR2 Expression During Bone Regeneration. *Front. Physiol.* **2019**, *10*, 512. [CrossRef]
21. Manescu, A.; Giuliani, A.; Mohammadi, S.; Tromba, G.; Mazzoni, S.; Diomede, F.; Zini, N.; Piattelli, A.; Trubiani, O. Osteogenic potential of dualblocks cultured with human periodontal ligament stem cells: In vitro and synchrotron microtomography study. *J. Periodontal. Res.* **2016**, *51*, 112–124. [CrossRef] [PubMed]

22. Mazzoni, S.; Mohammadi, S.; Tromba, G.; Diomede, F.; Piattelli, A.; Trubiani, O.; Giuliani, A. Role of Cortico-Cancellous Heterologous Bone in Human Periodontal Ligament Stem Cell Xeno-Free Culture Studied by Synchrotron Radiation Phase-Contrast Microtomography. *Int. J. Mol. Sci.* **2017**, *18*, 364. [CrossRef] [PubMed]
23. Wang, F.; Yu, M.; Yan, X.; Wen, Y.; Zeng, Q.; Yue, W.; Yang, P.; Pei, X. Gingiva-derived mesenchymal stem cell-mediated therapeutic approach for bone tissue regeneration. *Stem Cells Dev.* **2011**, *20*, 2093–2102. [CrossRef] [PubMed]
24. Xu, Q.C.; Wang, Z.G.; Ji, Q.X.; Yu, X.B.; Xu, X.Y.; Yuan, C.Q.; Deng, J.; Yang, P.S. Systemically transplanted human gingiva-derived mesenchymal stem cells contributing to bone tissue regeneration. *Int. J. Clin. Exp. Pathol.* **2014**, *7*, 4922–4929. [PubMed]
25. Yang, H.; Gao, L.N.; An, Y.; Hu, C.H.; Jin, F.; Zhou, J.; Jin, Y.; Chen, F.M. Comparison of mesenchymal stem cells derived from gingival tissue and periodontal ligament in different incubation conditions. *Biomaterials* **2013**, *34*, 7033–7047. [CrossRef] [PubMed]
26. Trubiani, O.; Orsini, G.; Zini, N.; Di Iorio, D.; Piccirilli, M.; Piattelli, A.; Caputi, S. Regenerative potential of human periodontal ligament derived stem cells on three-dimensional biomaterials: A morphological report. *J. Biomed. Mater. Res.* **2008**, *87*, 986–993. [CrossRef] [PubMed]
27. Trubiani, O.; Zalzal, S.F.; Paganelli, R.; Marchisio, M.; Giancola, R.; Pizzicannella, J.; Bühring, H.J.; Piattelli, M.; Caputi, S.; Nanci, A. Expression profile of the embryonic markers nanog, OCT-4, SSEA-1, SSEA-4, and frizzled-9 receptor in human periodontal ligament mesenchymal stem cells. *J. Cell. Physiol.* **2010**, *225*, 123–131. [CrossRef]
28. Silvestro, S.; Chiricosta, L.; Gugliandolo, A.; Pizzicannella, J.; Diomede, F.; Bramanti, P.; Trubiani, O.; Mazzon, E. Extracellular Vesicles Derived from Human Gingival Mesenchymal Stem Cells: A Transcriptomic Analysis. *Genes (Basel)* **2020**, *11*, 118. [CrossRef]
29. Tomar, G.B.; Srivastava, R.K.; Gupta, N.; Barhanpurkar, A.P.; Pote, S.T.; Jhaveri, H.M.; Mishr, G.C.; Wani, M.R. Human gingiva-derived mesenchymal stem cells are superior to bone marrow-derived mesenchymal stem cells for cell therapy in regenerative medicine. *Biochem. Biophys. Res. Commun.* **2010**, *393*, 377–383. [CrossRef]
30. Vizoso, F.J.; Eiro, N.; Cid, S.; Schneider, J.; Perez-Fernandez, R. Mesenchymal stem cell secretome: Toward cell-free therapeutic strategies in regenerative medicine. *Int. J. Mol. Sci.* **2017**, *18*, 1852. [CrossRef]
31. Pawitan, J.A. Prospect of stem cell conditioned medium in regenerative medicine. *BioMed. Res. Int.* **2014**, *2014*, 965849. [CrossRef] [PubMed]
32. Osugi, M.; Katagiri, W.; Yoshimi, R.; Inukai, T.; Hibi, H.; Ueda, M. Conditioned media from mesenchymal stem cells enhanced bone regeneration in rat calvarial bone defects. *Tissue Eng. Part A* **2012**, *18*, 1479–1489. [CrossRef] [PubMed]
33. Inukai, T.; Katagiri, W.; Yoshimi, R.; Osugi, M.; Kawai, T.; Hibi, H.; Ueda, M. Novel application of stem cell-derived factors for periodontal regeneration. *Biochem. Biophys. Res. Commun.* **2013**, *430*, 763–768. [CrossRef] [PubMed]
34. Katagiri, W.; Osugi, M.; Kinoshita, K.; Hibi, H. Conditioned medium from mesenchymal stem cells enhances early bone regeneration after maxillary sinus floor elevation in rabbits. *Implant Dent.* **2015**, *24*, 657–663. [CrossRef]
35. Katagiri, W.; Watanabe, J.; Toyama, N.; Osugi, M.; Sakaguchi, K.; Hibi, H. Clinical study of bone regeneration by conditioned medium from mesenchymal stem cells after maxillary sinus floor elevation. *Implant Dent.* **2017**, *26*, 607–612. [CrossRef]
36. Jing, H.; He, X.; Zheng, J. Exosomes and regenerative medicine: State of the art and perspectives. *Transl. Res.* **2018**, *196*, 1–16. [CrossRef]
37. Hao, Z.C.; Lu, J.; Wang, S.Z.; Wu, H.; Zhang, Y.T.; Xu, S.G. Stem cell-derived exosomes: A promising strategy for fracture healing. *Cell Prolif.* **2017**, *50*, e12359. [CrossRef]
38. Qin, Y.; Wang, L.; Gao, Z.; Chen, G.; Zhang, C. Bone marrow stromal/stem cell-derived extracellular vesicles regulate osteoblast activity and differentiation in vitro and promote bone regeneration in vivo. *Sci. Rep.* **2016**, *6*, 1–11. [CrossRef]
39. Furuta, T.; Miyaki, S.; Ishitobi, H.; Ogura, T.; Kato, Y.; Kamei, N.; Miyado, K.; Higashi, Y.; Ochi, M. Mesenchymal stem cell-derived exosomes promote fracture healing in a mouse model. *Stem Cells Transl. Med.* **2016**, *5*, 1620–1630. [CrossRef]

40. Zhang, S.; Chu, W.C.; Lai, R.C.; Lim, S.K.; Hui, J.H.; Toh, W.S. Exosomes derived from human embryonic mesenchymal stem cells promote osteochondral regeneration. *Osteoarthr. Cartil.* **2016**, *24*, 2135–2140. [CrossRef]
41. Werth, S.; Urban-Klein, B.; Dai, L.; Höbel, S.; Grzelinski, M.; Bakowsky, U.; Czubayko, F.; Aigner, A. A low molecular weight fraction of polyethylenimine (PEI) displays increased transfection efficiency of DNA and siRNA in fresh or lyophilized complexes. *J. Control. Release* **2006**, *112*, 257–270. [CrossRef] [PubMed]
42. Diomede, F.; Rajan, T.S.; Gatta, V.; D'Aurora, M.; Merciaro, I.; Marchisio, M.; Muttini, A.; Caputi, S.; Bramanti, P.; Mazzon, E.; et al. Stemness maintenance properties in human oral stem cells after long-term passage. *Stem Cells Int.* **2017**, *2017*, 5651287. [CrossRef] [PubMed]
43. Gugliandolo, A.; Diomede, F.; Cardelli, P.; Bramanti, A.; Scionti, D.; Bramanti, P.; Trubiani, O.; Mazzon, E. Transcriptomic analysis of gingival mesenchymal stem cells cultured on 3D bioprinted scaffold: A promising strategy for neuroregeneration. *J. Biomed. Mater. Res. Part A* **2017**, *106*, 126–137. [CrossRef] [PubMed]
44. Rajan, T.S.; Giacoppo, S.; Trubiani, O.; Diomede, F.; Piattelli, A.; Bramanti, P.; Mazzon, E. Conditioned medium of periodontal ligament mesenchymal stem cells exert anti-inflammatory effects in lipopolysaccharide-activated mouse motoneurons. *Exp. Cell Res.* **2016**, *349*, 152–161. [CrossRef] [PubMed]
45. Rajan, T.S.; Giacoppo, S.; Diomede, F.; Ballerini, P.; Paolantonio, M.; Marchisio, M.; Piattelli, A.; Bramanti, P.; Mazzon, E.; Trubiani, O. The secretome of periodontal ligament stem cells from MS patients protects against EAE. *Sci. Rep.* **2016**, *6*, 38743. [CrossRef] [PubMed]
46. Trubiani, O.; Marconi, G.D.; Pierdomenico, S.D.; Piattelli, A.; Diomede, F.; Pizzicannella, J. Human Oral Stem Cells, Biomaterials and Extracellular Vesicles: A Promising Tool in Bone Tissue Repair. *Int. J. Mol. Sci.* **2019**, *20*, 4987. [CrossRef] [PubMed]
47. Angelini, G.; Boncompagni, S.; De Maria, P.; De Nardi, M.; Fontana, A.; Gasbarri, C.; Menna, E. Layer-by-layer deposition of shortened nanotubes or polyethylene glycol-derivatized nanotubes on liposomes: A tool for increasing liposome stability. *Carbon* **2007**, *45*, 2479–2485. [CrossRef]
48. Angelini, G.; Boncompagni, S.; De Maria, P.; Fontana, A.; Gasbarri, C.; Siani, G. Kinetic evaluation of the effect of layer by layer deposition of polyelectrolytes on the stability of POPC liposomes. *Colloids Surf. Physicochem. Eng. Asp.* **2008**, *322*, 234–238. [CrossRef]
49. Paganin, D.; Mayo, S.C.; Gureyev, T.E.; Miller, P.R.; Wilkins, S.W. Simultaneous phase and amplitude extraction from a single defocused image of a homogeneous object. *J. Microsc.* **2002**, *206*, 33–40. [CrossRef]
50. Giuliani, A.; Iezzi, G.; Mozzati, M.; Gallesio, G.; Mazzoni, S.; Tromba, G.; Zanini, F.; Piattelli, A.; Mortellaro, C. Bisphosphonate-related osteonecrosis of the human jaw: A combined 3D assessment of bone descriptors by histology and synchrotron radiation-based microtomography. *Oral Oncol.* **2018**, *82*, 200–202. [CrossRef]
51. Weitkamp, T.; Haas, D.; Wegrzynek, D.; Rack, A. ANKAphase: Software for single-distance phase retrieval from inline X-ray phase-contrast radiographs. *J. Synchrotron Radiat.* **2011**, *18*, 617–629. [CrossRef] [PubMed]
52. Roschger, P.; Paschalis, E.P.; Fratzl, P.; Klaushofer, K. Bone mineralization density distribution in health and disease. *Bone* **2008**, *42*, 456–466. [CrossRef] [PubMed]
53. Niu, Z.; Pang, R.T.K.; Liu, W.; Li, Q.; Cheng, R.; Yeung, W.S.B. Polymer-based precipitation preserves biological activities of extracellular vesicles from an endometrial cell line. *PLoS ONE* **2017**, *12*, e0186534. [CrossRef] [PubMed]
54. Giuliani, A.; Iezzi, G.; Mozzati, M.; Gallesio, G.; Mazzoni, S.; Tromba, G.; Zanini, F.; Piattelli, A.; Mortellaro, C. Three-dimensional microarchitecture and local mineralization of human jaws affected by bisphosphonate-related osteonecrosis. *Oral Oncol.* **2018**, *84*, 128–130. [CrossRef] [PubMed]